AIP Journal of Applied Physics

Enhanced ferroelectric photovoltaic response of BiFeO3/BaTiO3 multilayered structure

Savita Sharma, Monika Tomar, Ashok Kumar, Nitin K. Puri, and Vinay Gupta

Citation: Journal of Applied Physics **118**, 074103 (2015); doi: 10.1063/1.4928964
View online: http://dx.doi.org/10.1063/1.4928964
View Table of Contents: http://scitation.aip.org/content/aip/journal/jap/118/7?ver=pdfcov
Published by the AIP Publishing

Enhanced ferroelectric photovoltaic response of $BiFeO_3/BaTiO_3$ multilayered structure

Savita Sharma,[1,2] Monika Tomar,[3] Ashok Kumar,[4] Nitin K. Puri,[2] and Vinay Gupta[1,a)]
[1]*Department of Physics and Astrophysics, University of Delhi, Delhi 110007, India*
[2]*Department of Applied Physics, Delhi Technological University, Delhi 110042, India*
[3]*Physics Department, Miranda House, University of Delhi, Delhi 110007, India*
[4]*CSIR-National Physical Laboratory, Dr. K. S. Krishnan Marg, Delhi 110012, India*

(Received 31 March 2015; accepted 8 August 2015; published online 21 August 2015)

The present work is based on the photovoltaic properties of multilayered structure of Bismuth ferrite (BFO) and Barium titanate (BTO) thin films prepared by pulsed laser deposition technique on platinum coated silicon substrate. The multilayered structure possesses enhanced ferroelectric properties and shows a remarkable increase in photocurrent (from 1.56×10^{-7} A to 6.96×10^{-5} A) upon illumination with laser light of wavelength 405 nm at an intensity of 160 mW/cm^2. The values of short circuit photocurrent and open circuit voltage were found to be 0.3184 mA/cm^2 and −1.25 V, respectively, with a light-to-electricity conversion efficiency of 0.067%. A relatively high efficiency calculated at 405 nm for the developed multilayered BFO/BTO structure highlights its practical application in ferroelectric photovoltaics. © *2015 AIP Publishing LLC*.
[http://dx.doi.org/10.1063/1.4928964]

I. INTRODUCTION

Over several decades, researchers have been striving to open different corridors for the production of renewable energy to curb the evolving demands for inexhaustible energy and clean fuel sources.[1–5] The exceptional advantages of ferroelectric photovoltaic effect (FE-PV) over the conventional p-n junction based photovoltaic (PV) devices, such as high output voltage and polarization controlled PV response, appear promising for the realization of efficient functional devices.[1,6–8] FE-PV effect is observed in several perovskite oxide systems, such as $Pb(Zr,Ti)O_3$ (PZT), $BaTiO_3$ (BTO), etc.,[3,7–10] but disappointingly, the photovoltaic efficiency in such materials undergoes quenching due to their small current density (of the order of 10^{-9} A/m^2) and large optical band gap (typically ∼3.5 eV). Therefore, it becomes imperative to tailor the physiochemical properties of these ferroelectric materials for possible device applications.

Most notable of the available ferroelectric materials, Bismuth ferrite (BFO) with its small optical band gap and good chemical stability, has fueled interest of the research community in past several years. Moreover, the lead free nature of BFO does not constrict its potential applications as compared to its non-environment friendly counterpart, lead zirconium Titanate (PZT).[6] BFO is a room temperature multiferroic material having high ferroelectric Curie temperature (∼1120 K) and antiferromagnetic Neel temperature (∼643 K).[11–13] However, the inherent high leakage current reduces its ferroelectric polarization and hence is a major concern for onward applications.[2]

Several reports are available on A-site and B-site doping for improving the ferroelectric properties of BFO thin films[13,14] as well as on the study of tip enhanced photovoltaic properties of BFO.[15] Gupta *et al*. discussed the effect of doping at "A" and "B" sites in BFO and reported a remarkable enhancement in photovoltaic properties but the efficiency was still compromised.[16] Doping may induce unwanted parasitic phase formation which restricts any enhancement of FE-PV effect. Hence, it is important to come up with strategic ideologies to fully exploit the potential material traits for obtaining an enhanced response in BFO.

On the other hand, BTO is an equally attractive perovskite ferroelectric material employed in various devices, including capacitors, ferroelectric memories, etc., due to its unique dielectric, piezoelectric, and ferroelectric properties.[5,9,17] However, BTO, being a wide band gap (∼3.3 eV) semiconductor, cannot be employed for FE-PV applications, especially in the visible spectral region. Reportedly, multilayered structures possess superior ferroelectric properties compared to individual parent materials in terms of high polarization, high dielectric constant, and relatively lower losses.[14] Thus, in order to improve the ferroelectric properties of BFO while simultaneously reducing the band gap of BTO, fabrication of the multilayered structure of BFO and BTO could be beneficial.

There are several reports where band gap engineering has been demonstrated by fabricating layered thin film structure.[18,19] Some research groups have also studied BFO/BTO multilayered structures, but their photovoltaic properties are scarcely reported.[20,21] Toupet *et al*.[22] and Yang *et al*.[23] examined the multiferroic property of the BFO/BTO multilayered structure and conclusively reported an improvement in the magnetic property of the system. There exists a correlation between the phenomena of ferroelectricity and photoconductivity observed in certain materials. Ferroelectric polarization acts as a driving force for the separation of photo-generated charge carriers within a photovoltaic cell. When light with a wavelength corresponding to the energy

a)Electronic addresses: vgupta@physics.du.ac.in and drguptavinay@gmail.com

band gap of the ferroelectric thin film is made incident on it, photon energy is utilized for the generation of charge carriers—electrons and holes. The photo-generated electrons and holes are driven by the polarization-induced internal electric field in opposite directions and thus, contribute to the photovoltaic output. A BFO-BTO integrated system might result in a composite with effectively lower band gap and high ferroelectric polarization (i.e., low leakage current) which could then be utilized for the realization of an efficient FE-PV device. In the present study, a BFO/BTO multilayered structure has been prepared on Pt(111)/Ti/SiO_2/Si(100) substrate using pulsed laser deposition (PLD) technique and its structural, optical, ferroelectric, and PV properties have been studied in detail.

II. EXPERIMENTAL

A BFO/BTO multilayered (five layered) structure was prepared by PLD technique. Single phase 1 in. diameter ceramic targets of BFO and BTO were prepared via conventional solid state reaction method using Bi_2O_3, Fe_2O_3, $BaCO_3$, and TiO_2 (99.9% pure) as precursor materials. 20% excess Bi was used in the BFO target to avoid the Bi loss during high temperature processing due to its volatile nature. The powders for BFO and BTO were separately ball-milled, dried, and pressed into discs followed by sintering at 850 °C and 1250 °C, respectively. The targets were then polished and mounted on target holders for the deposition of thin films.

The targets were ablated sequentially using the 4th harmonic of Nd:YAG pulsed laser ($\lambda = 266$ nm) and a multilayered structure of BFO/BTO was prepared on Pt/Ti/SiO_2/Si substrate. A 70 nm thin layer of Pt metal was deposited over the passivated Si (SiO_2/Si) substrate by E-beam evaporation technique. A buffer layer of Ti (20 nm) was deposited *in-situ* over SiO_2/Si substrate prior to Pt deposition to improve the adhesion of Pt. Typical deposition parameters used for deposition of BFO and BTO thin films are summarized in Table I.

Total thickness of the multilayered structures was kept fixed at 350 nm, while thickness of individual layers of BFO and BTO was about 70 nm. The multilayered structure was prepared at a substrate temperature of 750 °C. Thickness of individual layers and multilayered structure was measured using surface profiler (Dektak 150). The number of layers in the multilayered structure was kept fixed to be five, keeping BTO as the bottom layer. The ferroelectric measurements were made in metal-ferroelectric-metal (MFM) configuration where Pt layer deposited on SiO_2/Si substrate was considered as the bottom electrode. The top circular electrodes (600 μm diameter, 40 nm thickness) of Au were deposited by thermal evaporation technique through a shadow mask on the surface of multilayered BFO/BTO structure. The schematic of MFM capacitor configuration (Au/BTO/BFO/…/BTO/Pt/SiO_2/Si) is shown in Fig. 1. For comparison, thin films of both BFO and BTO of same thickness (350 nm) were also grown under similar deposition conditions on Pt/SiO_2/Si substrate. For studying the optical properties, thin films were deposited on fused quartz substrate.

TABLE I. PLD processing conditions for the growth of BFO/BTO multilayered structure.

Parameters	Deposited conditions
Ceramic targets	20% Bi-excess BFO, BTO (1 in. diameter)
Substrate	Pt/Ti/SiO_2/Si
Substrate temperature	750 °C
Deposition pressure	200 mT
T-S distance	4.5 cm
Laser type	Nd:YAG (266 nm)
Fluence	120 mJ
Thickness of BTO and BFO	70 nm

Structural characterization of prepared samples was carried out using X-ray diffraction (XRD) analysis (Bruker D8). The lattice parameters of BFO and BTO thin films in the multilayered thin film structure were calculated by Le-Bail fitting using Bruker Topas 3 software. Optical properties were studied using UV-Visible spectrophotometer (Perkin Elmer Lambda 35). A radiant technology precision ferroelectric workstation was used to measure the room temperature ferroelectric polarization (PE hysteresis) of the prepared samples at a frequency of 1 kHz and at an applied bias of 10 V. For the photovoltaic measurements, the BFO/BTO multilayered sample was illuminated with violet laser light ($\lambda = 405$ nm) and the current-voltage (I-V) characteristics of prepared samples were monitored using Keithley (4200) semiconductor characterization system.

III. RESULTS AND DISCUSSIONS

Figure 2 shows the XRD pattern of the prepared five layered BTO/BFO structure. For comparison, XRD patterns of the single layer BFO and BTO thin films (350 nm thin) fabricated under identical conditions on Si substrates have also been included. It may be seen that all prepared samples are polycrystalline in nature depicting rhombohedral distorted structure for BFO and tetragonal structure for BTO. XRD pattern of the BFO/BTO multilayered structure (Fig. 2) reveals that all the observed peaks correspond to either BFO or BTO phases only. Absence of any extra XRD peak in all

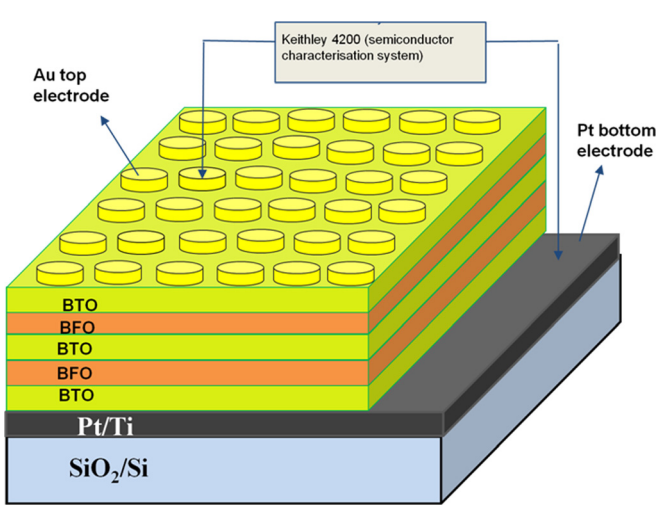

FIG. 1. Schematic of the MFM capacitor configuration of the BFO/BTO multilayer structure.

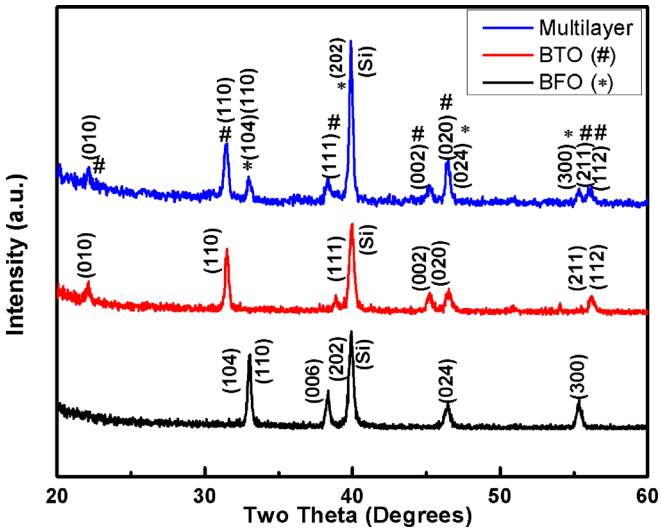

FIG. 2. XRD pattern of BFO/BTO multilayered structure. XRD pattern of bare BFO and BTO thin films is also included for comparison.

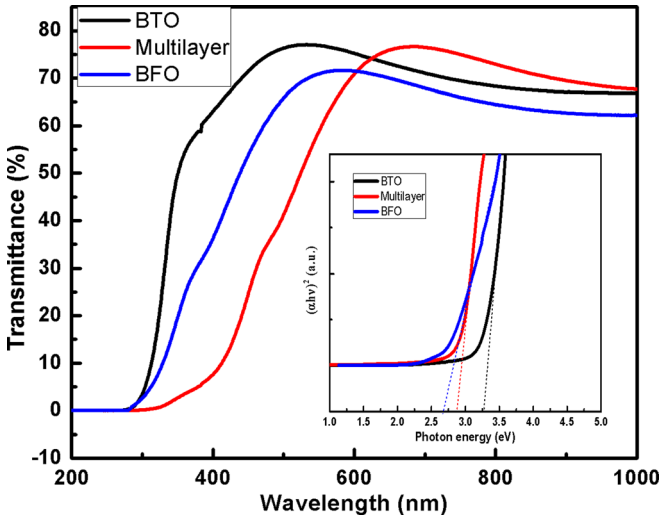

FIG. 3. UV-Visible transmission spectra of bare BTO film, bare BFO film, and BFO/BTO multilayered structure. Inset shows the Tauc plot of all the three prepared samples.

prepared samples clearly rules out the possibility of formation of any impure secondary phase. Furthermore, two XRD peaks around $2\theta = 45°$ corresponding to BTO can be easily observed for the multilayered structure (Fig. 2), indicating that BTO possesses a tetragonal structure. Lattice parameters ("a" and "c"), unit cell volume "V," and stress modulus for both BTO and BFO in the multilayered structure were determined using LeBail Intensity Extraction method with the help of Bruker TOPAS 3 Software and are summarized in Table II. For comparison, the corresponding bulk values for BTO and BFO are also included in Table II [JCPDS card No. 01-072-0138 and 01-072-2035]. The estimated values of lattice parameters a and c are 4.38 Å and 4.07 Å, respectively, for BTO film and 5.53 Å and 13.54 Å, respectively, for BFO film. These values are slightly lower than the corresponding reported values for bulk BFO but greater than that of bulk BTO (Table II), indicating the introduction of tensile and compressive stress, respectively, in BTO and BFO thin films in the multilayered structure. The stress modulus in both layers is calculated using the equation, stress $= |(c_o - c)|/c_o$ in %, where "c" is the lattice constant of BFO or BTO thin film in multilayered structure and "c_o" is the corresponding bulk value. The value of stress modulus (%) for BTO and BFO was found to be about 1.11% and 2.04%, respectively. A large value of stress modulus present in the BFO thin film indicates a large lattice distortion which may lead to improved ferroelectric property.

Figure 3 shows the optical transmission spectra of multilayered BFO/BTO structure deposited on quartz substrate over a wavelength range of 190–1100 nm. The transmission spectra of bare BFO and BTO thin films are also included in Fig. 3 for comparison. It can be seen from Fig. 3 that the bare BFO and BTO thin films were highly transparent (~80%) in the visible region demonstrating the growth of thin films with good optical quality and low absorption losses. However, transmittance in the case of multilayered structure drops to 70% (Fig. 3) and may be due to refraction of light at the multiple interfaces. The Tauc plot of $(\alpha h\nu)^2$ versus photon energy ($h\nu$) (where α is absorption coefficient, h is Planck's constant, and ν is frequency of the incident radiation) of the multilayered structure and bare thin films is shown in the inset of Fig. 3. The estimated values of bandgap for all the prepared samples are also summarized in Table III. Optical bandgap of the multilayered structure as calculated from the extrapolation of linear region in Tauc plot is about 2.87 eV which is much less than that of pure BTO (3.27 eV) thin film and close to that of BFO thin film (2.66 eV). It can be easily seen from Table III that the integration of BFO with BTO has indeed helped in reducing the band gap of the overall multilayered structure and is suitable for ferroelectric photovoltaic applications.

Figure 4 shows the typical ferroelectric P-E hysteresis loop of the mutilayered BFO/BTO structure at an applied bias of 10 V and 1 kHz frequency. For comparison, hysteresis loops of bare BTO and BFO thin films grown under similar conditions have also been included in Fig. 4. It may be seen from Fig. 4 that the ferroelectric properties of the multilayered BFO/BTO structure are better in comparison to that of

TABLE II. Lattice parameters "a" and "c," cell volume "V" and stress modulus for BFO and BTO thin films in BFO/BTO multilayer (five layer) structure.

	BTO thin film					BFO thin film				
	Lattice parameter		Volume	Stress modulus	c/a distortion	Lattice parameter		Volume	Stress modulus	c/a distortion
	a (Å)	c (Å)	V $(Å)^3$	(%)	ratio	a (Å)	c (Å)	V $(Å)^3$	(%)	ratio
Bulk value	3.999	4.033	64.36	—	1.0085	5.876	13.867	374.94	—	2.3599
multilayer	4.381	4.078	77.661	1.11	0.9308	5.5301	13.584	358.82	2.04	2.4563

TABLE III. Ferroelectric parameters and band gap of multilayered BFO/BTO sample. The corresponding values for bare BFO and BTO thin films are also included for comparison.

	P_r ($\mu C/cm^2$)	P_s ($\mu C/cm^2$)	$2E_c$ (kV/cm)	E_g (eV)
BTO	43.28	74.82	4.85	3.27
BFO	12.23	20.61	5.35	2.66
Multilayer	45.71	64.69	11.27	2.87

bare BFO thin film and comparable to the bare BTO thin film. The obtained values of remnant polarization (P_r), saturation polarization (P_s), and coercive field (E_c) for all the structures are summarized in Table III. The multilayered system exhibits a saturation polarization (P_s) of around 64.69 $\mu C/cm^2$, which is much greater than that obtained for bare BFO thin film (20.61 $\mu C/cm^2$). The value of $P_s = 64.69\ \mu C/cm^2$ and $P_r = 45.71\ \mu C/cm^2$ obtained for multilayered BFO/BTO structure in the present work is relatively higher in comparison to the corresponding values reported by various workers for multilayered structure of BFO with other materials or doped BFO thin film.[2,6,13,14,24] The improved ferroelectric property of the multilayered structure may be related to the stress induced at the interfaces. Furthermore, the observed slight asymmetry in the hysteresis loops (Fig. 4) is attributed to the presence of different top and bottom metal (Pt and Au) electrodes in MFM structure. It may be noted that the presence of BFO and BTO films in the multilayered structure results in a lower bandgap and higher ferroelectric polarization, making the fabricated multilayered structure suitable for ferroelectric photovoltaic applications.

Figure 5 shows the current density–voltage (J–V) curve obtained for multilayered BFO/BTO sample under both dark condition and light illumination ($\lambda = 405$ nm). The J–V curve under light illumination (Fig. 5) shows a typical ferroelectric photovoltaic effect. The photovoltaic open-circuit voltage (V_{oc}) and short-circuit current density (J_{sc}) are found to be about -1.25 V and 0.3184 mA/cm^2, respectively, as

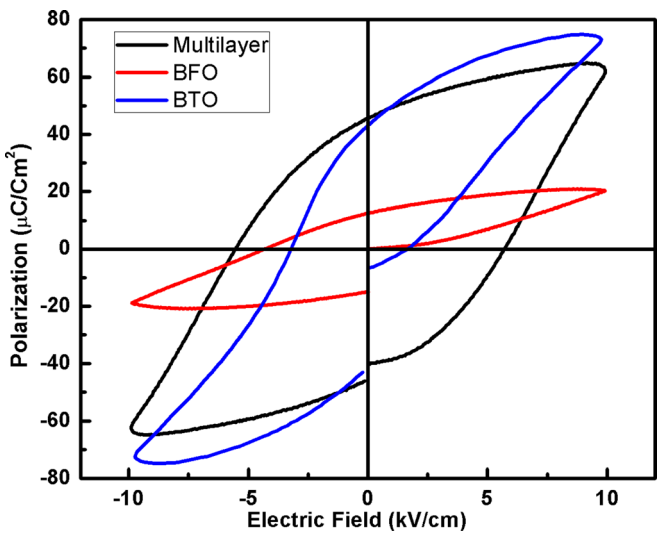

FIG. 4. Room temperature ferroelectric (P-E) hysteresis curves of bare BFO and BTO thin films and multilayered BFO/BTO structure.

determined from the intercept on the horizontal and the vertical axes (Fig. 5). The photovoltage obtained is considerably larger than that reported by other researchers for individual ferroelectric thin films.[9,16,24–26] It is well known that the value of J_{SC} and V_{OC} for ferroelectric thin films under illumination depends on the internally generated electric field. The internal electric field in ferroelectric thin films is given as $E = E_{bi} + E_p$, where E_{bi} is the built-in field and E_p is the depolarization field. The built in field E_{bi} in ferroelectric thin films is driven by various factors.[27–29] The depolarization field E_p is directly proportional to the strength of polarization: $E_p = \frac{-P}{\varepsilon_o \varepsilon_F}\left(\frac{2\varepsilon_F/d}{2\varepsilon_F/d+\varepsilon_e/\lambda}\right)$, where ε_F *is* the relative dielectric constant of the ferroelectric thin film, ε_e is the relative dielectric constant of the electrode layer, λ is the screening length, P is the polarization value, and d is the thickness of ferroelectric thin film.[4] Therefore, high photovoltaic output obtained for BFO/BTO multilayered structure can be attributed to its higher internal field caused by the larger remnant polarization (Fig. 4). The large depolarization field could effectively separate the photogenerated electrons and holes and hence, resulting in enhanced photovoltaic output for BFO/BTO multilayered structure. Inset of Fig. 5 shows the transient response characteristics of photocurrent density measured at zero bias for multilayered BFO/BTO structure under continuous on and off conditions of laser light ($\lambda = 405$ nm) at a regular interval of 20 s. The photoresponse of multilayered BFO/BTO structure shows a rapid increase in the photocurrent with illumination on its surface, and subsequently saturates at a constant value (inset of Fig. 5). When the incident light is turned off, the photocurrent decreases rapidly and reaches its original value. Now to compare the photovoltaic response of BFO/BTO multilayered structure with that of BFO single layer, photovoltaic measurement on BFO single layer was performed and is shown in Figure 5(b). A very small open circuit voltage and short circuit current ($V_{oc} = -0.33$ V and $J_{sc} = 1.30 \times 10^{-4}$ A/cm^2) are generated in the case of single layer BFO thin film. On the other hand, BTO with its wide band-gap energy (3.27 eV as calculated) which is larger than the energy corresponding to 405 nm wavelength exhibits no absorption of the incident energy. Hence, BTO thin film failed to exhibit photovoltaic effect at this wavelength of 405 nm and thus photovoltaic response is not included for BTO single layer. In the case of multilayered structure, the presence of BFO is crucial due to its band gap compatibility in correspondence with the wavelength of incident light ($\lambda = 405$ nm), whereas BTO induces an internal field in response to the large polarization, thereby accelerating the separation of photogenerated charge carriers. Collectively BFO/BTO multilayered system exhibits an enhanced photovoltaic response at 405 nm as compared to single layered BFO or BTO.

The photocurrent responsivity, i.e., ratio of the short circuit photocurrent density (Acm^{-2}) to the input optical power density (mWcm^{-2}) is also calculated for the multilayered BFO/BTO structure from the J-V curve and is estimated to be about 1.99 mAW^{-1} at an input power of 160 mWcm^{-2}. Light-to-power conversion efficiency, η, can be determined

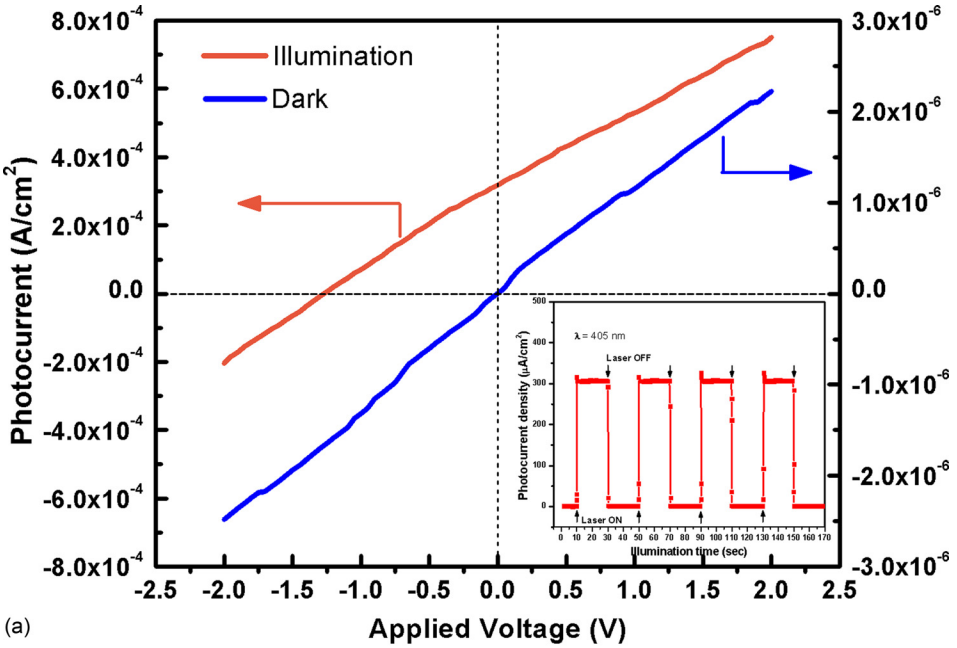

(a)

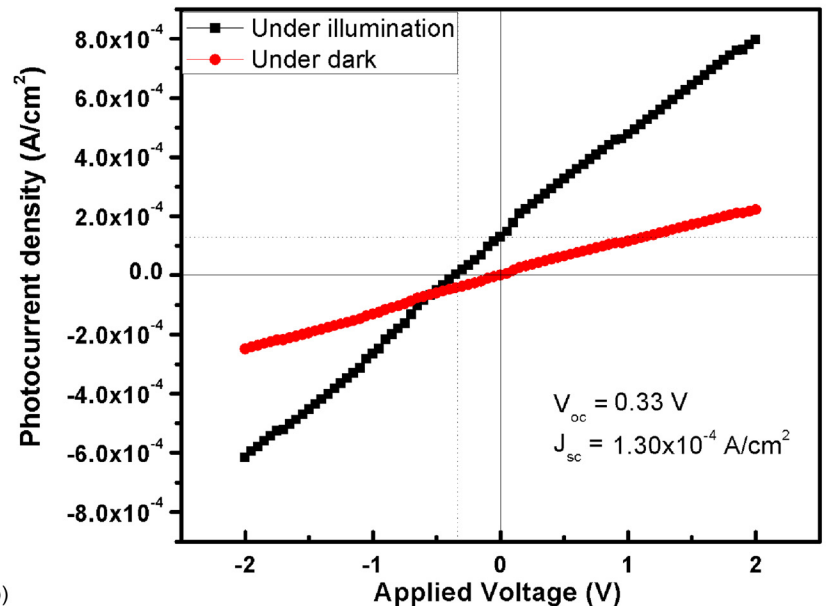

(b)

FIG. 5. (a) J-V curves for multilayered BFO/BTO structure under both dark condition and illumination of light. Inset shows transient response of short circuit photocurrent density of multilayered BFO/BTO structure when laser beam is switched on and off at regular intervals of 20 s. (b) J-V curve for BFO single layer thin film under both dark condition and illumination of light to compare the photovoltaic response with BFO/BTO multilayer structure.

from the J-V curve obtained under photo illumination. We calculated the power conversion efficiency of the investigated structure at 405 nm. The power conversion efficiency η is the ratio of the output electrical power density (P_{out}) to the input optical power density (P_{in}). The input power density, P_{in} ($mWcm^{-2}$) is the intensity of light incident on the surface of the sample and the output power density, P_{out} ($mWcm^{-2}$) at a certain point (J,V) of the J-V curve is the area enclosed by the point (J,V) and two axes (i.e., $P_{out} = JV$ mW/cm^2). The power conversion efficiency η at the point (J,V) can be calculated as[16] $\eta = \frac{Pout}{Pin} = \frac{JV}{Pin}$.

The voltage dependence of power conversion efficiency of the multilayered BFO/BTO structure is presented in Fig. 6. It can be observed from Fig. 6 that the maximum power conversion efficiency (0.067%) occurs at half the value of open circuit photovoltage. The power conversion efficiency is associated with the separation and subsequent

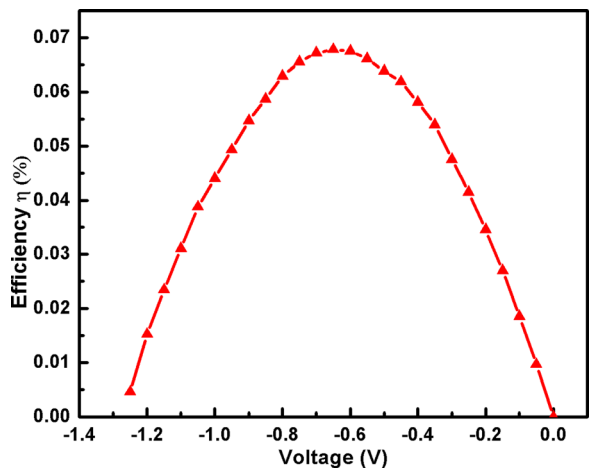

FIG. 6. The variation of power conversion efficiency calculated at 405 nm as a function of applied voltage for BFO/BTO multilayer structure.

movement of polarization led photogenerated charge carriers. The higher value of remnant polarization of the multilayered BFO/BTO structure provides a large internal electric field (depolarization field) which acts as a driving force that separates the photogenerated electron-hole carriers resulting in higher power conversion efficiency.[4] The power conversion efficiency calculated at 405 nm in the case of developed BFO/BTO multilayered structure is higher compared to the photovoltaic efficiency reported recently for BFO.[16,26,30] However, there are few reports where higher power conversion efficiency compared to that observed in the present work has also been reported.[4] It was identified that when ITO was used as a top electrode, more absorption of incident photons in the visible region occurred. The open circuit voltage and short circuit current for multilayered BFO/BTO structure are -1.25 V and 3.184×10^{-4} A/cm^2, respectively.

It may be inferred that the prepared multilayered BFO/BTO structure exhibits a large remnant polarization ($45.71\ \mu$C/cm^2) and hence high photovoltaic output that makes it attractive for photovoltaic applications.

IV. CONCLUSION

Multilayered structure having five alternating layers of single phase BFO and BTO thin films was deposited using PLD technique. Multilayered BFO/BTO structure exhibits a good ferroelectric hysteresis loop with high saturation polarization, $P_s = 64.69\ \mu$C/Cm^2 and remnant polarization, $P_r = 45.71\ \mu$C/Cm^2. The low optical band gap coupled with the high ferroelectric polarization results in good ferroelectric photovoltaic response of BFO/BTO multilayered structure. The short circuit photocurrent density and open circuit voltage are about $9.96\ \mu$A/cm^2 and -1.25 V, respectively. The light-to-electricity power conversion efficiency calculated at 405 nm is relatively high (0.067%). The enhanced photovoltaic response observed in present work is attributed to the presence of strong depolarization field due to higher remnant polarization and lower band gap of the multilayered BFO/BTO structure. The obtained results show that the prepared BFO/BTO multilayered system could be used efficiently for energy harvesting and other photovoltaic applications.

ACKNOWLEDGMENTS

Authors are thankful to Department of Science and Technology (DST) and University of Delhi for the financial support. One of the authors (S.S.) is thankful to the Delhi Technological University (DTU) for the teaching assistantship.

[1]S. Y. Yang, J. Seidel, S. J. Byrnes, P. Shafer, C.-H. Yang, M. D. Rossell, P. Yu, Y.-H. Chu, J. F. Scott, J. W. Ager III, L. W. Martin, and R. Ramesh, Nat. Nanotechnol. **5**, 143 (2010).
[2]S. Y. Yang, L. W. Martin, S. J. Byrnes, T. E. Conry, S. R. Basu, D. Paran, L. Reichertz, J. Ihlefeld, C. Adamo, A. Melville, Y.-H. Chu, C.-H. Yang, J. L. Musfeldt, D. G. Schlom, J. W. Ager III, and R. Ramesh, Appl. Phys. Lett. **95**, 062909 (2009).
[3]J. Zhang, X. Su, M. Shen, Z. Dai, L. Zhang, X. He, W. Cheng, M. Cao, and G. Zou, Nat. Sci. Rep. **3**, 2109 (2013).
[4]B. Chen, M. Li, Y. Liu, Z. Zuo, F. Zhuge, Q. F. Zhan, and R. W. Li, Nanotechnology **22**, 195201 (2011).
[5]W. Cai, C. Fu, J. Gao, Q. Guo, X. Deng, and C. Zhang, Physica B **406**, 3583 (2011).
[6]Z. Lin, W. Cai, W. Jiang, C. Fu, C. Li, and Y. Song, Ceram. Int. **39**, 8729 (2013).
[7]K. Yao, B. K. Gan, M. Chen, and S. Shannigrahi, Appl. Phys. Lett. **87**, 212906 (2005).
[8]M. Qin, K. Yao, and Y. C. Liang, Appl. Phys. Lett. **93**, 122904 (2008).
[9]W. Jiang, W. Cai, Z. Lin, and C. Fu, Mater. Res. Bull. **48**, 3092 (2013).
[10]L. Chen, B. C. Luo, N. Y. Chan, J. Y. Dai, M. Hoffman, S. Li, and D. Y. Wang, J. Alloys Compd. **587**, 339 (2014).
[11]J. F. Ihlefeld, N. J. Podraza, Z. K. Liu, R. C. Rai, X. Xu, T. Heeg, Y. B. Chen, J. Li, R. W. Collins, J. L. Musfeldt, X. Q. Pan, J. Schubert, R. Ramesh, and D. G. Schlom, Appl. Phys. Lett. **92**, 142908 (2008).
[12]S. Gupta, M. Tomar, and V. Gupta, J. Exp. Nanosci. **8**(3), 261 (2013).
[13]H. W. Chang, F. T. Yuan, Y. C. Yu, P. C. Chen, C. R. Wang, C. S. Tu, and S. U. Jen, J. Alloys Compd. **574**, 402 (2013).
[14]N. M. Murari, A. Kumar, R. Thomas, and R. S. Katiyar, Appl. Phys. Lett. **92**, 132904 (2008).
[15]M. Alexe and D. Hesse, "Tip-enhanced photovoltaic effects in bismuth ferrite," Nat. Commun. **2**(256), 1–4 (2011).
[16]S. Gupta, M. Tomar, and V. Gupta, J. Appl. Phys. **115**, 014102 (2014).
[17]Y. H. Chen, W. H. Tuan, and J. Shieh, J. Eur. Ceram. Soc. **30**, 2577 (2010).
[18]H. K. Yadav, K. Sreenivas, and V. Gupta, Appl. Phys. Lett. **96**, 223507 (2010).
[19]H. K. Yadav, K. Sreenivas, and V. Gupta, Appl. Phys. Lett. **90**, 172113 (2007).
[20]S. Sharma, M. Tomar, A. Kumar, N. K. Puri, and V. Gupta, Physica B **448**, 125 (2014).
[21]M. Lorenz, V. Lazenka, P. Schwinkendorf, F. Bern, M. Ziese, H. Modarresi, A. Volodin, M. J. V. Bael, K. Temst, A. Vantomme, and M. Grundmann, J. Phys. D: Appl. Phys. **47**, 135303 (2014).
[22]H. Toupet, V. V. Shvartsman, F. Lemarrec, P. Borisov, W. Kleemann, and M. Karkut, Integr. Ferroelectr. **100**, 165 (2008).
[23]P. Yang, K. M. Kim, J. Y. Lee, J. Zhu, and H. Y. Lee, Integr. Ferroelectr. **113**, 26 (2010).
[24]R. S. Katiyar, P. Misra, S. Sahoo, G. Morell, and R. S. Katiyar, J. Alloys Compd. **609**, 168 (2014).
[25]W. Dong, Y. Guo, B. Guo, H. Liu, H. Li, and H. Liu, Mater. Lett. **91**, 359 (2013).
[26]W. Dong, Y. Guo, B. Guo, H. Liu, H. Li, and H. Liu, Mater. Lett. **88**, 140 (2012).
[27]K. Abe, N. Yanase, T. Yasumoto, and T. Kawakubo, J. Appl. Phys. **91**(1), 323 (2002).
[28]D. J. Kim, J. Y. Jo, Y. S. Kim, Y. J. Chang, J. S. Lee, J. G. Yoon, T. K. Song, and T. W. Noh, Phys. Rev. Lett. **95**, 237602 (2005).
[29]A. Gruverman, A. Kholkin, A. Kingon, and H. Tokumoto, Appl. Phys. Lett. **78**, 2751 (2001).
[30]S. Gupta, M. Tomar, A. Kumar, and V. Gupta, Adv. Sci. Lett. **20**, 971–976(6) (2014).